Journal of Geoscience and Environment Protection, 2024, 12, 207-231
https://www.scirp.org/journal/gep
ISSN Online: 2327-4344
ISSN Print: 2327-4336

Granulometry Assessment of Lom Pangar Dam Sediments (East-Cameroon)

Rodrigue Fotie Lele[1,2*], Mihaela Amalia Diminescu[3], Issoufou Ouedraogo[1,4], Annette Madelene Dăncila[3], Souleymane Pelede[1], Alphonse Emadak[5], Martin Lompo[1]

[1]Department of Geology, University Joseph Ki Zerbo, Ouagadougou, Burkina Faso
[2]Department of Water and Energy, Green Heart International, Bafoussam, Cameroon
[3]Department of Hydraulic Machineries and Environmental Engineering, National University of Science and Technology Politehnica Bucharest, Bucharest, Romania
[4]Department of Mining Engineering, University Yembila-Abdoulaye-Toguyeni, Fada N'Gourma, Burkina Faso
[5]Department of Inorganic Chemistry, University of Yaoundé I, Yaoundé, Cameroon
Email: *rodrigue.fotie@ujkz.bf, *fotielelerodrigue@gmail.com

How to cite this paper: Fotie Lele, R., Diminescu, M. A., Ouedraogo, I., Dăncila, A. M., Pelede, S., Emadak, A., & Lompo, M. (2024). Granulometry Assessment of Lom Pangar Dam Sediments (East-Cameroon). *Journal of Geoscience and Environment Protection, 12,* 207-231.
https://doi.org/10.4236/gep.2024.126013

Received: April 26, 2024
Accepted: June 24, 2024
Published: June 27, 2024

Abstract

The Lom Pangar dam, the largest reservoir in Cameroon with a storage capacity of 6 km^3 and a 30 MW hydropower plant, primarily regulates the hydrologic regime of the Sanaga River to maintain hydropower efficiency during dry seasons and enhance downstream hydropower plant performance. Understanding and managing sediments are crucial for the sustainability of dams, as indicated by numerous studies. This study assessed the granulometry of the sediments transported across the reservoir. For that purpose, 6 samples of fresh sediments were collected in the lacustrine and transitional sections of the reservoir using the standard method. Particles size was assessed using the laser diffusion technic after a 3 mm sieving. Various granulometric parameters were derived from the literature to analyze and characterize those sediments. Results show that silts are more than 70% of particles size and range between 2.19 - 60.26 µm. Size distribution also shows the same trend with D_{75} less than 51 µm. This is confirmed by the low values of Inman Skewness $Sk\Phi$ (−0.168 to 0.303). The Sorting index S_0 ranges from 0.31 to 0.53 µm, showing a *very well-sorted sediments*, aligning with low values of Krumbein index (0.906 - 1.683) that express the *low heterometry* of the particles. The consequence on the dam will be a quick clogging of the bottom of the reservoir. Their pH varies from 7.0 to 7.5. It also appears that the sandy fraction trend is higher in the right bank of the dam and reaches 22% on the right bank of Pangar River due to crystalline geology. Fraction greater than 3000 µm is negligible. The management of the dam has to keep attention to these results as siltation may close the safety outlet of the dam, damage turbines, and provoke recurrent technical and safety issues. Further, the clogging

of the bottom of the reservoir may lead to an ecological problem with the limitation of hyporheic flow. Thus, water exchange with the underground water table and the natural purification of water reduce, while increasing sediments deposits change the biogeochemistry processes.

Keywords

Lom Pangar Dam, Sediments Granulometry, Sustainability, Hydropower, Dam Safety

1. Introduction

1.1. Context

The Lom Pangar dam (Lom Pangar) is the largest dam built in Cameroon. Situated approximately 120 km north of Bertoua, the capital of the eastern region, the project was initiated by the Government of Cameroon in response to an unprecedented energy crisis around 2002 and was officially launched in early 2010. The reservoir is 53 m high and was impounded for the 1st time in 2016 to reach its storage capacity of 6 km^3 and its surface area of 532 km^2 (Guillemot et al., 2017). The 30 MW power plant installed at the toe of the dam was launched in January 2024. Various environmental and social mitigation measures were implemented, including secondary activities such as fishing, aimed at enhancing the benefits of the Lom Pangar (EDC, 2016; Emadak et al., 2019a).

Preserving the quality of inputs into the reservoir is crucial for maintaining water quality and the proper functioning of hydropower equipment such as turbines and mechanical components of the dam. The development of riparian villages, artisanal mining, and all human activities in the watershed may, if they are not controlled, significantly affect the quality of the input in the reservoir (Emadak et al., 2019b). Sediments play an important role in transporting substances and distributing contaminants in water, as well as in potentially damaging mechanical equipment or reducing storage capacity (Kummu et al., 2010; Ousmanou, 2020; Schleiss et al., 2008; Sharma & Gandhi, 2023; Taylor, 2007).

Reservoir sedimentation poses a significant challenge for water resources management, with approximately one percent of reservoir capacity being lost each year (Antoine et al., 2020; Schleiss et al., 2008). Globally, reservoir sediment retention is estimated at around 30% (Vörösmarty et al., 2003) and predictions suggest a potential 60% loss in storage capacity by 2040 (Oehy, 2003). This indicates that newly constructed reservoirs worldwide already have less storage capacity than what is lost due to sedimentation, adding to erosion, abrasion, and corrosion that are common issues encountered in hydropower plants.

1.2. Problem Statement

Erosion by sediments of hydro-turbines and their components presents a significant challenge (Singh, 2021). Decreases turbine performance increases both the

time and cost of maintenance. From an ecological perspective, the sedimentation of fine particles poses a threat to fish populations, endangering their habitats and main trophic resources (Bănăduc et al., 2020). Clogging of streambed sediment caused by the infiltration of fine particles at depth reduces the hydraulic conductivity and hyporheic flow (Bendaoud et al., 2021). Therefore, the sediments of Lom Pangar, particularly their particle size, require careful attention.

1.3. Objective

This study aims to predict potential challenges that may arise in the long-term performance and sustainability of the Lom Pangar reservoir based on the dynamics of particle granulometry transported within the reservoir. The study assesses the particle size and their distribution within the reservoir.

2. Paper Review Summary

2.1. Geology of Lom Pangar

Geology of Lom Pangar watershed is dominated by anciens syn-tectonic granites as well as migmatitic and garnetiferous gneiss crossed by NE-SW oriented faults (Figure 1).

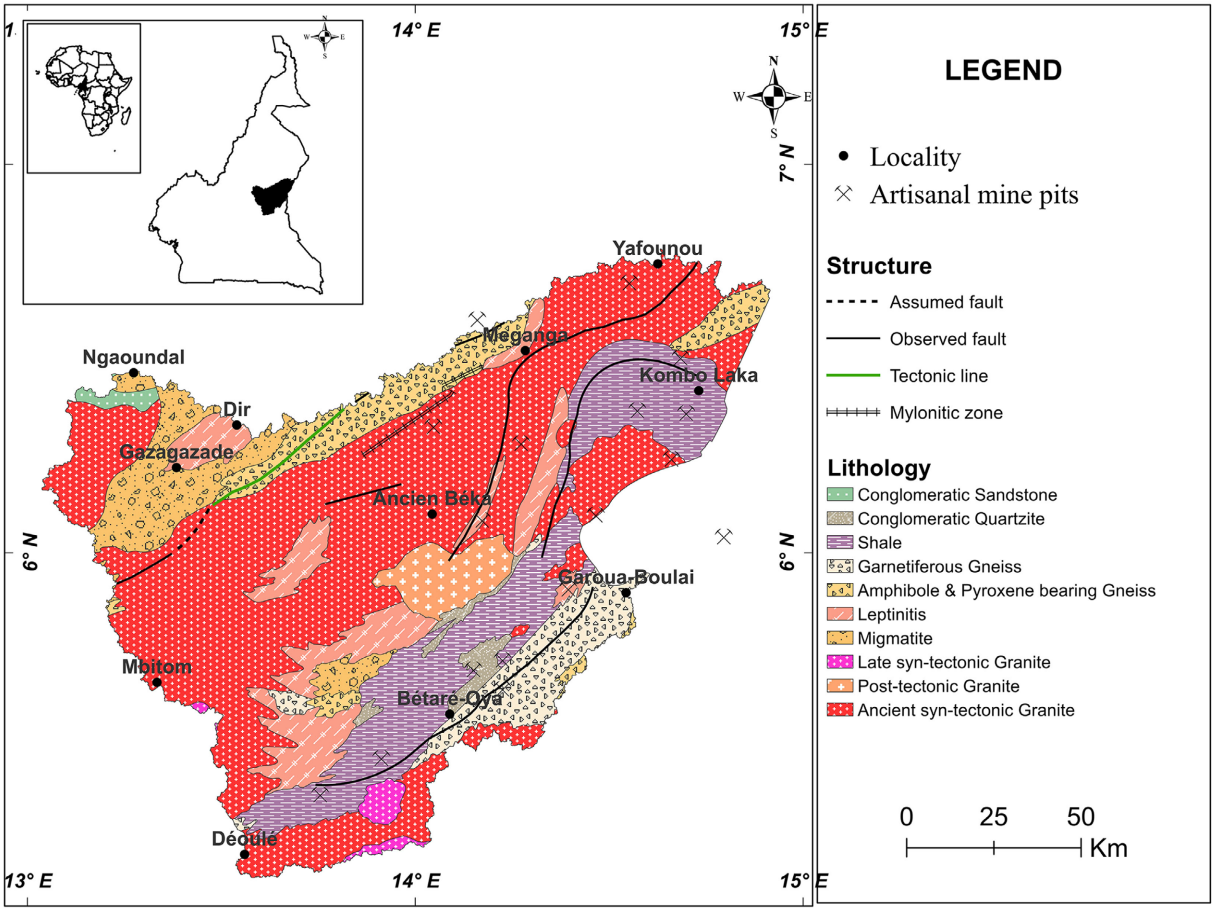

Figure 1. Geological map of Lom Pangar watershed. Modified from "Geological Map of the Unified Cameroon".

A band of gold mineralized shale, following the same orientation with mayor linar structures, appears in the SE of Lom Subwatershed and is subjected to prolific artisanal gold mining.

2.2. Influence of Particle Size

Particle size is a fundamental property of any sediment, soil, or dust deposit. It affects their entrainment, transport, and deposition, and therefore provides important clues to the sediment provenance, transport history, and depositional conditions (Pye & Blott, 2004; Wanogho et al., 1987). Particle size analysis provides a valuable method for characterizing soils and sediments, aiding in comparison and environmental interpretation (Chappell, 1998). Because of their large specific surface areas, particles like sand, silt, and clay, can play a significant role in adsorption processes in various environmental contexts as they have more sites available for adsorption. This means they can adsorb more molecules or ions. Finer particles, such as clay, have a larger surface area compared to coarser particles like sand. As a result, finer sediments often exhibit higher adsorption capacities (Garnier-Laplace et al., 1997).

The influence of sediment grain size on the magnetic parameters and heavy metal contents is strong (Abrahim & Parker, 2008; Li et al., 2011). Sediments could be a potential source of heavy metals that can be released into the overlying water via natural and anthropogenic processes, where they could harm the drinking water quality and human health (Pélédé et al., 2018; Suresh et al., 2012). Due to the weathering of rocks and anthropogenic activities, elements are produced and transported by Rivers and redistributed to adjacent lakes and their sediments. One of the most important processes affecting this migration of elements is interaction with geological materials. The accumulation and distribution of elements depend mostly on the characteristics of the geological material such as mineral species and grain sizes. The fine fraction (less than 62.5 μm) is consistently more contaminated than bulk samples (Taylor, 2007). Metals have low solubility in water and are adsorbed and accumulated on bottom sediments (Jain et al., 2008).

2.3. Sediments and Ecology

Lake sediments serve as fundamental components of our environments, providing essential nutrients for living organisms. They also act as sensitive indicators for monitoring contaminants, serving as both sinks and carriers for pollutants within the aquatic environment (Bai et al., 2011). Therefore, the analysis of lake sediments plays a crucial role in evaluating the pollution status of aquatic environments.

The hyporheic zone, which refers to the transitional area between the surface water of a river and the groundwater beneath (**Figure 2**), is an ecologically rich and dynamic region where surface water and groundwater interact.

This zone typically occurs in the sediment or substrate beneath the waterbed

that are characterized by a unique set of physical, chemical, and biological conditions. The hyporheic zone plays a vital role in various ecological processes (Schmutz & Moog, 2018; Seliger & Zeiringer, 2018; Touchette et al., 2015), including nutrient cycling, filtration of contaminants, and habitat for a diverse array of aquatic organisms. Additionally, it serves as a refuge for many species during periods of environmental stress, such as drought or extreme temperatures.

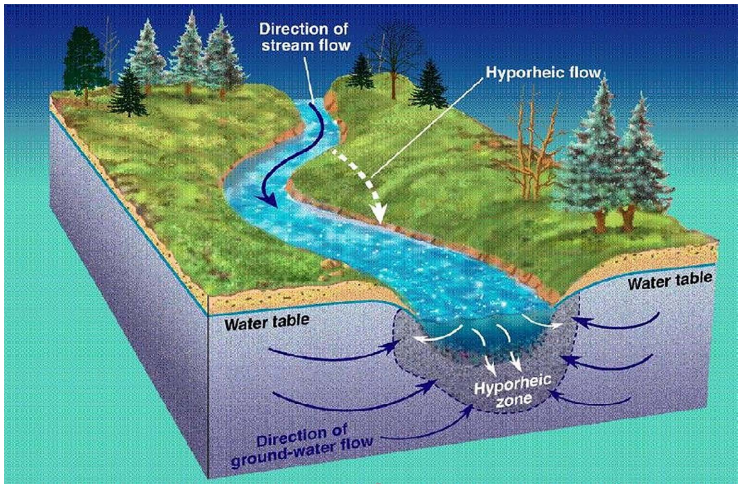

Figure 2. Illustration of the hyporheic zone with lateral and vertical exchanges with an alluvial plain (Touchette et al., 2015).

2.4. Sediments and Turbines Damaging

Sediments can damage turbines and other mechanical equipment through erosion of the coating on the blades (**Figure 3**), leading to surface irregularities and more serious material damage (Azrulhisham & Azri, 2018; Rai et al., 2020). One of the factors contributing to the gradual decline in the performance as well as the failure of hydropower plants over the years is silt erosion (Tandel et al., 2023).

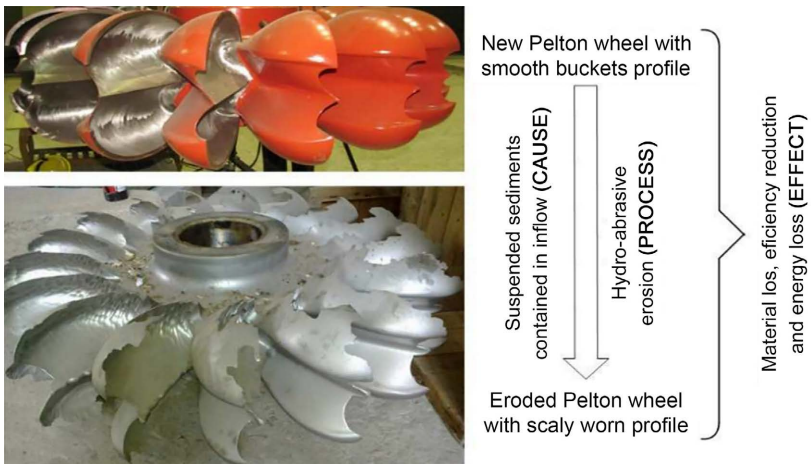

Figure 3. Hydro-abrasive erosion on a runner of a pelton (Rai et al., 2020).

Many other authors have also worked on the impact of sediment on turbines and mechanical equipment of dams (Sharma et al., 2021; Sharma & Gandhi, 2023; Tandel et al., 2023; Tarodiya et al., 2022).

Abrasive particles in the run-of-river hydropower plants reduce unit efficiency, increase maintenance costs, and may cause turbine downtime and associated production losses.

One of the factors contributing to the gradual decline in the performance as well as the failure of hydropower plants over the years is silt erosion. To deal with this situation during the design, operation, and maintenance of hydro plants, knowledge of turbine wear needs to be improved with regard to relevant suspended sediment parameters including the suspended sediment concentration (SSC) and particle size distribution (PSD). Measurements of SSC and PSD were conducted at the intake weir and settling basin of a run-of-river hydropower plant in Bentong, Malaysia, using Laser *In-Situ* Scattering and Transmissometry (LISST) instruments. The results indicate that all samples were predominantly composed of silt and fine sand particles, with a mean size range of less than 50 μm and concentrations ranging from 10 to 30 mg/l (Azrulhisham & Azri, 2018). The identification of the continental origin of the deposit suggests the need to develop solutions in the upper watershed to reduce the siltation rate (Amarjouf et al., 2015).

2.5. Laser Diffusion Granulometry

Laser diffusion is widely used as a particle size technique for materials ranging from a few hundred nanometers to several millimeters, typically from 0.02 μm to 2000 μm (**Figure 4**).

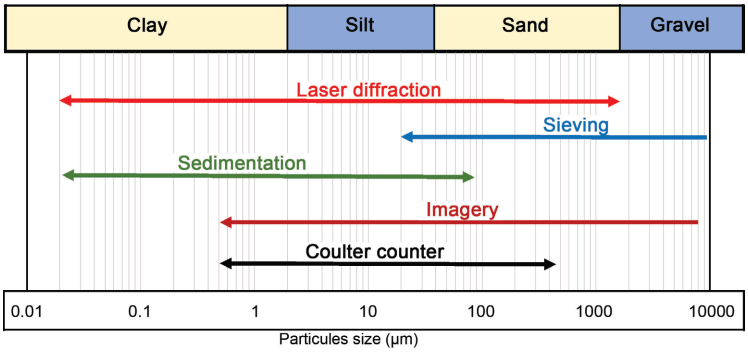

Figure 4. Measurable particle size ranges with different optimal particle size measuring techniques. Modified from (Delanghe et al., 2017).

When it comes to studying environments that contain a significant quantity of silt and clay, particle size analysis by laser diffraction was mainly developed since the end of the 1990s is the technique preferred to mechanical analyses based on the interactions between light and matter (Delanghe et al., 2017). The angles of light scattering by the analyzed particles depend on the particle size. It is thus possible to obtain in a few minutes an estimate of the particle size proportions of particles present in different types of samples (solid or liquid). This method also

makes it possible to work on smaller sample volumes than sieving.

3. Methodology

3.1. Study Area

The study area is shown in Figure 5. It belongs to the department of Lom and Djerem, East Region of Cameroon, at about 120 km N of the capital city of Bertoua. It is located between 05˚37'38" - 07˚22'40"N latitudes and 13˚26'25" - 14˚05'19"E longitudes, with an average altitude of 700 m.a.s.l. The site is part of the savannah tropical (Beck et al., 2018), commonly called sub-equatorial "Guinean" climate. Heavy rains fall from August to mid-December. The mean annual rainfall is 1578 mm/year. Temperatures are relatively constant over the year with an annual average of 23˚C ± 1˚C. Winds are low in the study site both in frequency and intensity. The "calm" period (≤1 m/s) represents 44% of the year. South-west winds dominating in the rainy season represent 26.3% of the time and the northern winds of the dry season 7.7%. Sampling sites have been chosen according to the longitudinal zonation of water quality conditions in the future reservoir with smooth shapes).

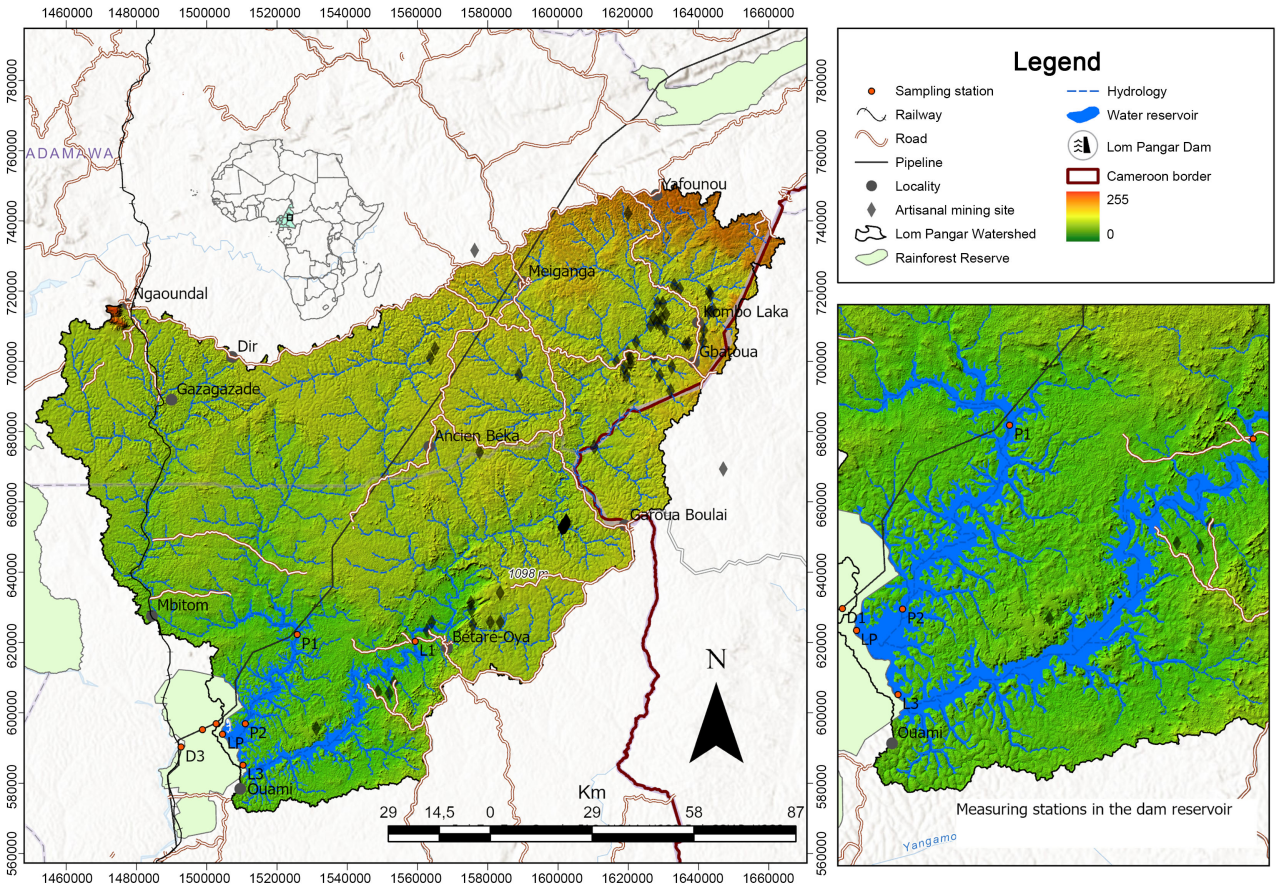

Figure 5. Map showing the Lom Pangar watershed and hydrography as well as sampling stations of the dam monitoring. (Stations used in this study are LP in the lacustrine section, P2 on the Pangar branch and L3 in the Lom Branch all in the transitional section of the Dam. They are less than 10 km from the dam outlet, turbines and mechanical equipment of the Dam. D1 is located 900 m downstream of the dam. outlet).

The study site consists of the transitional and lacustrine sections of the Lom Pangar. It belongs to a whole program of the dam monitoring with 8 sampling stations. The choice of the sections and stations used in this paper is because of their vicinity to the outlet of the dam that carries the turbines and mechanical equipment, as well as low water energy.

The other sections of the dam include the riverine with stations L1 and P1, and the downstream stations with D1, D2 and D3 are not considered in this article as the focus is on sediments reaching the outlet. L represents the Lom River. It's a major contributor to the Sanaga where the downstream stations D1, D2 and D3 are going. It rises in the Central Africa Republic, in the southeastern edge of Adamaoua, towards the 1400 m (Figure 6) and 70 km east of Meiganga, and flows down through the Adamaoua plateau with a difference in altitude of 590 m and slope up to 20%, to reach Sanaga River at 380 km downstream.

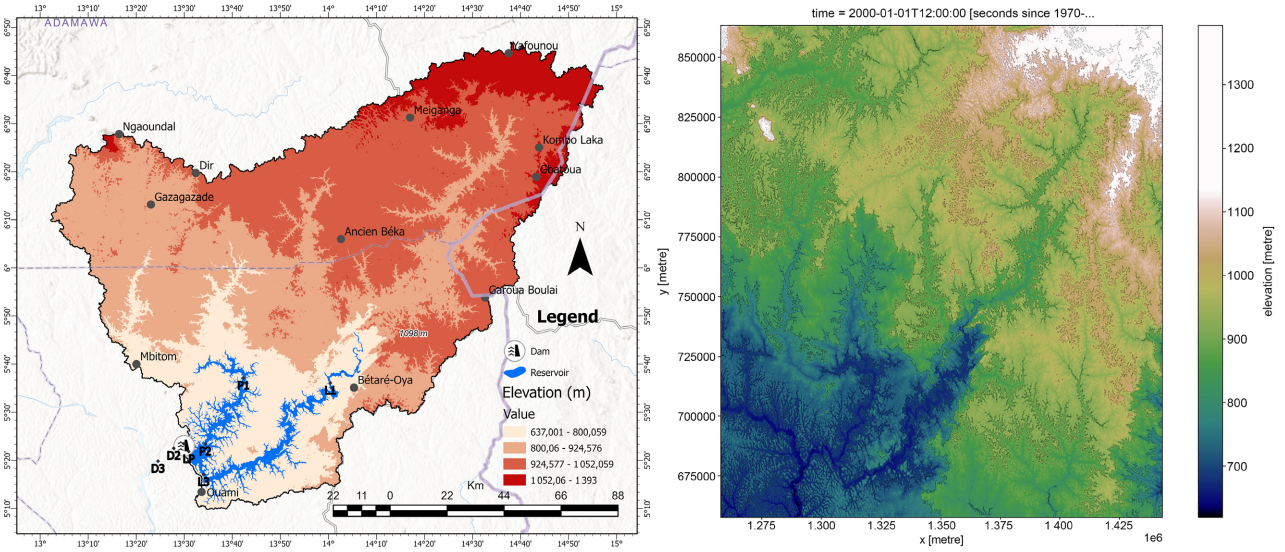

Figure 6. Terrain elevation image of the Lom Pangar watershed (left) and the sector covering the watershed (right). The Dam is located at the vicinity of 640 m.a.s.l. with a very low slope.

Its flow rates in low hydrologic regimes vary between 10 to 42 m^3/s over the year. Pangar River (P), the main tributary of Lom River (L), rises at the foot of the Ngaoundal in the western part of the Adamawa Plateau. P rises at over 100 km far and joins the Lom at around 5 km upstream of the site of the dam outlet.

3.2. Sampling and Analysis Process

- **Fresh shallow sediments sampling**

Sampling was conducted using the standard method outlined by AFNOR (2009) and AFNOR ISO 13320-1 (2009). A plastic shovel was used to collect swallow sediments on the tidal zone, at the water borders from 04 to 09 April 2023, with the beginning of the dam filling period. This period was chosen because of the closure of the dam weirs that further significantly reduces the speed of water flow to deposit more finer particles. Samples were collected from 6

points across 3 stations representing the transitional and lacustrine sections of the dam. Upon collection, each sample was immediately placed into sampling bags in bulk and gently squeezed to remove the excess of water. Subsequently, samples were properly conditioned and transferred to the laboratory of Physico-chemical Analysis in Environmental Engineering, at the Department of Hydraulic, Hydraulic Machines, and Environmental Engineering of the Faculty of Energy at the Politéhnica University of Bucharest, Romania.

- **Sample preparation**

Each sample was weighed and its pH measured using a pH-meter. Subsequently, the samples were dried in an oven at 40˚C to remove moisture, and their weight was recorded every 4 hours until the variation in mass became negligible. Dried samples were crushed (**Figure 7**), and sifted to obtain a fine and homogeneous powder. Sporadic large fragments and visible debris were picked out manually and the processed samples stored in clean and labeled containers. A fraction of 3 grams from each sample was transferred to the laboratory of Science and Engineering of Oxide Materials and Nanomaterials within the same university. Here, the samples underwent sieving using a 3 mm mesh to obtain the desired particle size.

Figure 7. Dried sample from the Oven (left), crushed to separate particles (middle) and the Malvern Instruments Mastersizer 2000 Measuring unit used for diffusion laser granulometry (right).

- **Laser diffusion particle size analysis**

The granulometric analysis was done on the finer sample fraction mixed in ethyl alcohol on the Laser Diffusion Technique with the Malvern Instruments Mastersizer 2000 © Measuring unit (**Figure 7**), following the manufacturer's prescription and standard methods (Delanghe et al., 2017; Fournier-Sowinski et al., 2012). Bulbs are removed in the system and the dispersion of aggregate into an ethyl alcohol milieu is done with a pump rotating at 2500 r/min. Three measures were done and the average value was taken.

4. Results and Discussion

However grain size analysis has been long time be a preferred approach for unconsolidated sediment characteristics, each data processing methods (statistic moments, textural analysis, multivariate statistics combining Principal Component Analysis and hierarchical cluster analysis, and CM image and end-member

modeling analysis) has it benefits and limitations mentioned from early work (Folk, 1966; Rivière, 1977) to actual (Duquesne & Carozza, 2023). Some parameters of those processing methods are displayed below and combine to understand the behavior of analysed sediments of Lom Pangar.

4.1. Laser Diffusion Insights Data

These data offer a comprehensive understanding of the characteristics and behavior of particles in a solution, which is crucial for particle characterization across diverse fields, including environmental science. Table 1 presents the detailed insights gleaned from laser diffusion samples analyzed during the study.

Table 1. Outcome of the laser analysis insights parameter and laboratory measured pH.

Parameter	E1-LPG	E2-LPD	E3-P2G	E4-P2D	E5-L3G	E6-L3D
Obscuration (%)	14.30	17.51	18.53	15.08	16.20	14.69
Particle Refractive Index (*PRI*)	1.650	1.650	1.650	1.650	1.650	1.650
Absorption K	0.1	0.1	0.1	0.1	0.1	0.1
Dispersant Refractive Index (*DRI*)	1.330	1.330	1.330	1.330	1.330	1.330
% Weighted Residual	4.914	2.763	1.240	1.095	0.639	1.356
%Vol concentration	0.0118	0.0136	0.0170	0.0157	0.0119	0.0095
Specific surface area (m^2/g)	0.961	1.020	0.876	0.765	1.070	1.21
pH	7.2	7.0	7.2	7.5	7.1	7.2

- **Obscuration (%)**

The obscuration percentage provides insight into the degree of light scattering or absorption by particles in the solution. The optimal obscuration range that provided the best measurement performance is set in the table and is between the normal known range (10% - 20%). In this case, values above 20% suggest a higher concentration of particles or larger particle sizes, which can impact the clarity or opacity of the solution. Thus, the highest value (18.5%) in the sample E3-P2G may be due to the influence of it coarser grain tendency observed at the right bank of the River Pangar.

- **Particle Refractive Index**

The Particle Refractive Index (PRI) indicates how much particles bend or refract light. It appears consistent at 1.650. Consistent values across samples suggest uniformity in particle composition or size, while variations may indicate differences in particle properties. Thus, each sample analysed is consistent in its particle properties such as its mineral component.

- **Absorption K**

The absorption coefficient represents the extent to which particles absorb light at a specific wavelength. Its value is 0.1 and appears low and consistant for all

samples. Higher values of this parameter suggest greater light absorption, which could be due to factors like particle composition or size distribution. It corroborates with the above-mentioned PRI that displays each sample as consistent in properties.

- **Dispersant Refractive Index**

The Dispersant Refractive Index (DRI) is consistent here with a single low value of 1.330, close to the above-mentioned PRI for all samples which is also a single low value 1.650 for all sample. For a dispersant medium, it shows how light interacts with suspended particles and helps appreciate the quality of the results of the lazer diffusion. Matching or closely aligned values between DRI and PRI optimize dispersion stability and minimize light scattering. Thus the ethyl alcohol used as dispersant in the analysis optimised the stability of the milieu for best refraction of particles.

- **Weighted Residual percentage**

This parameter indicates the level of deviation between observed and expected values in a model or analysis. Values range between 0.639 on a sample E5-L3G and 4.914% on a sample E1-LPG. Lower values suggest a better fit of the model to the data, indicating a more accurate characteristic of particle properties. Thus, a relatively high value on sample E1-LPG may be due to its relatively coarse grain tendency.

- **Volume concentration percentage**

The Volume concentration reflects the proportion of the solution occupied by particles. Changes in concentration can affect various properties such as viscosity, optical properties, and stability of colloidal suspensions. This parameter is very low and ranges between 0.0095% and 0.0170%. Thus, all sample analysis milieu are close in terms of concentration and fit with initial analysis parameters.

- **Specific surface area of sediment**

Specific surface area measures the extent of particle a surface relative to its mass. This represents the total surface area per unit mass of the sediment particles. It is an important parameter for understanding various physical, chemical, and biological processes occurring at the sediment water interface. Fine-grained sediments generally have higher specific surface areas compared to coarse-grained sediments due to their larger surface area per unit mass. Generally, higher values indicate larger surface area available for interactions, such as adsorption, chemical reactions, or agglomeration, which can influence particle behavior and performance in various applications. But this is not the case at the Lom Pangar given their range between 0.765 m^2/g for E4-P2G to 1.21 m^2/g in E6-L3D with high-value trends in the left bank (finer grain size trend). This corroborates with the fact that the specific surface area of sediment can vary widely depending on many factors such as particle size distribution, mineralogy, surface roughness, and porosity. Thus, it appears that geology with particle roughness and mineralogy may have played a major role on the parameter and this aspect keeps attention to

carrying further studies to understand.

4.2. Position Parameters

Table 2 displays the insights data into the particle size distribution of the sample being analyzed such as quartiles, percentiles, and statistics parameters.

Table 2. Position parameters of the sediments.

Parameter	E1-LPG	E2-LPD	E3-P2G	E4-P2D	E5-L3G	E6-L3D
D10 (µm)	2.228	2.195	2.504	2.935	2.113	1.999
D16 (µm)	2.75	2.65	3.00	3.98	2.21	2.37
D25 (µm)	4.20	4.00	4.85	6.41	3.99	3.38
D50 (µm)	**13.897**	**12.365**	**15.252**	**15.751**	**11.606**	**8.761**
D75 (µm)	14.74	24.00	50.00	31.50	21.50	26.30
D84 (µm)	83.50	37.50	150.00	47.00	26.30	20.10
D90 (µm)	123.773	55.147	244.714	81.386	39.926	30.149
D95 (µm)	NA	NA	NA	NA	NA	NA
D99 (µm)	NA	NA	NA	NA	NA	NA
Span	8.746	4.283	15.881	4.420	3.258	3.213
Uniformity	2.56	1.33	4.19	1.46	1.39	1.04
Mode	15.14	17.38	7.59	19.95	17.38	15.14
Surface weighted Mean $D[3, 2]$	6.241	5.859	6.851	7.839	5.611	4.960

Not Applicable (D_{95} is neglectable as well as indices using it when clayed fraction is greater than 10%).

- **Median Diameter D_{50}**

The median diameter represents the particle size at which 50% of the cumulative distribution is below that size. It describes the central tendency of the particle size distribution and gives an estimation of the average coarseness of the sediment by integrating all the particle size classes. It varies between 8.761 µm in E6-L3D and 15.751 µm in E4-P2D µm. Thus sediments analyzed are dominated by clays and finer silts. However, as mentioned in paragraph 4, this parameter is perfect only with the unimodal distribution and might deviate if particule are bimodal or multimodal distribution (White et al., 2007).

- **Mode**

The mode defines the size of sieves that have a maximum particle. It represents de size with the maximum concentration ratio of the particles. In sediment granulometry, the mode refers to the particle size that appears most frequently within a sample. Unlike the median or mean, which represent central tendencies, the mode identifies the most common size class or size range in the sediment. River Pangar mentioned the lowest values at the right bank E3-P2G (7.59) and the higher values at the left bank E4-P2D to 19.95. However, the Particles size distribution frequency curve (Figure 10), described later on section 4.4, dis-

plays multimodal particle sizes explaining the tendency of particle to differentiate more or less into specific class sizes.

- **Surface weighted mean particle size $D[3, 2]$**

The surface weighted mean particle size is expressed as the surface mean diameter of particles. It is particularly useful when considering properties of materials that are influenced by surface area, such as reactivity, dissolution rate, or surface adsorption. It expresses the average particle size of the sample from the Equation (1):

$$D[3,2] = \frac{\sum\left(D_i^3 \cdot S_i\right)}{\sum\left(D_i^2 \cdot S_i\right)} \tag{1}$$

where:

D_i is the diameter of the individual particle i and S_i the surface associated with particle i.

$D[3, 2]$ values are very low and range from 4.960 μm in the E6-L3D to 7.839 μm in E4-P2G confirming the dominant fraction of clays and finer silts in sediments.

In application, this formula is highly accurate only in the conditions of spherical particles and homogenous material (particles and composition) and narrow size distribution (Li et al., 2005). When samples deviate much from these conditions, accuracy may also deviate. Further, the accuracy of the analysis technique is to be considered, especially when particles tend to agglomerate or aggregate and make the interpretation of the results more complex as it may not be accurately reflecting the true $D[3, 2]$. However, despite these limitations, it remains a valuable parameter for characterizing particle size distributions, especially in applications where surface area plays a crucial role. It's often used in conjunction with other particle size parameters to provide a comprehensive understanding of particle size characteristics.

- **Uniformity Index or Span**

The Span measures the width of the particle size distribution and indicates the uniformity or spread of particle size within the sample. It is calculated in the Equation (2).

$$\text{Span} = \frac{D_{90} - D_{10}}{D_{50}} \tag{2}$$

where:

D_{90} is the diameter below which 90% of the cumulative volume distribution is found,

D_{10} is the diameter below which, 10% of the cumulative volume distribution is found,

D_{50} is the median diameter or the diameter below which 50% of the cumulative volume distribution is found.

This dimensionless quantity varies between 3.213 in E6-L3D and 15.881 in E3-P2G. A smaller value indicates a narrower particle size distribution, suggest-

ing that the majority of particles in the sample are of similar sizes. The high-value trend of the Span is registered in the right band of the dam with the Pangar tributary. These observations corroborate with other parameters. As per the D_{50}, this parameter is perfectly accurate in the case of unimodal distribution and less in the multimodal differentiated distribution as analysed samples.

- **Uniformity:**

Uniformity is assessed by examining how closely the particle size distribution resembles a single peak or distribution curve, indicating a more uniform distribution of particle sizes. It refers to the degree of consistency or homogeneity in particle size distribution class within the sample. A more uniform particle size distribution suggests that the sediment sample contains particles that are relatively similar in size, without significant variations or outliers. Values greater than zero here, vary from 1.04 at E6-L3D to 4.19 at E3-P2G. The high value in the right bank of the dam showing the heterogeneity trend of the grain size might be due to the coarser particle trend noticed on that bank. It should be noted that the geology of the Pangar subwatershed is mostly crystalline and may have produce the coarser trend of sandy particles than the Lom containing a band of gold shale-bearing, source of artisanal mining, but both subwatershed have the same elevation level. The Lom spring source is in the Central Africa Republic.

4.3. Particle Size Fractions

- **Coarse particle fraction**

Fraction greater than 3000 μm obtained after sieving is displayed in Table 3.

Table 3. Coarse fraction of the transitional and lacustrine sections of Lom Pangar sediments.

Size (μm)	E1-LPG (%)	Cumul E1-LPG	E2-LPD (%)	Cumul E2-LPD	E3-P2G (%)	Cumul E3-P2G	E4-P2D (%)	Cumul E4-P2D	E5-L3G (%)	Cumul E5-L3G	E6-L3D (%)	Cumul E6-L3D
>3000	4.80	4.80	0.00	0.00	2.60	2.60	4.60	4.60	2.30	2.30	11	11
<3000	95.20	100.00	100.00	100.00	97.40	100.00	95.40	100.00	97.70	100.00	89.00	100.00

LP, P and L stand for study stations. E stands for collected samples, Cumul stands for cumulative granulometry.

This fraction is negligible in regard to their low percentage in the total bulk sample (Figure 8). A relative high concentration (11%) is met at the sample E6-L3D. The point is located less than 1 km downstream of the River access point from the Ouami village. The relatively high concentration should be due to the coastal erosion from population activities, mainly board river access for a river crossing for fishing and traveling in that section of the river. Apart from that sample, it appears that the right band of the dam is seen to provide coarser particles than the left band as mentioned.

The low proportion of coarse particles can be explained by the change in transportation conditions. As they are mainly transported by cartage, a transport threshold should be reached, particularly for non-cohesive sediments (Powell & Soares Frazao, 2017; Swartenbroekx et al., 2013; White et al., 1975). This included the flow rate of the river, the slope of the topography, the falling speed of

particles, the roughness of the water bed and the characteristics of the particle itself. Such particle characteristics are the equivalent diameter, density, particle morphology and granulometric distribution.

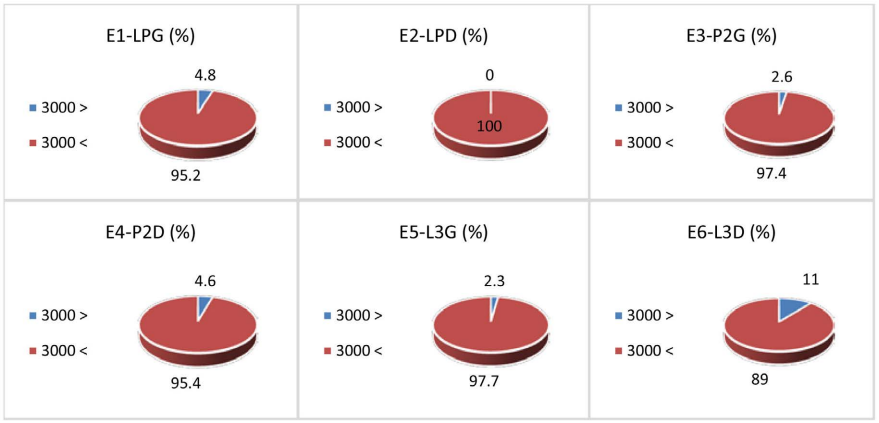

Figure 8. Proportion of the coarse and fine particles of Lom Pangar Lacustrine and Transitional sections.

The Lom Pangar dam is located in the low altitude of the watershed with a very low slope (**Figure 6**). This combined with the fact that sampling was done at the beginning of the dam filling, contributes to slow the river flow rates towards the subcritical regimes with high loss of its specific energy. This phenomenon was observed in Dupuyer Creek, Montana, USA (Whitaker & Potts, 2007) and in the Lower Mekong River in Viet Nam (Bravard et al., 2014).

- **Fine particle size fraction**

This constitutes the major fraction of Lom Pangar sediment. They are composed of Silt > Clay > Sand, as displayed in **Table 4**.

Table 4. Fine sediments of Lom Pangar dam.

Class (µm)	Size (µm)	E1-LPG (%)	Cumul E1-LPG	E2-LPD (%)	Cumul E2-LPD	E3-P2G (%)	Cumul E3-P2G	E4-P2D (%)	Cumul E4-P2D	E5-L3G (%)	Cumul E5-L3G	E6-L3D (%)	Cumul E6-L3D
Clay < 2	0.55	0.00	0.00	0.00	0.00	0.00	0.00	0.00	0.00	0.00	0.00	0.00	0.00
	0.63	0.00	0.00	0.00	0.00	0.00	0.00	0.00	0.00	0.00	0.00	0.00	0.00
	0.72	0.12	0.12	0.09	0.09	0.09	0.09	0.09	0.09	0.14	0.14	0.10	0.10
	0.83	0.57	0.69	0.57	0.66	0.39	0.48	0.42	0.51	0.71	0.85	0.68	0.78
	0.96	0.96	1.65	1.08	1.74	0.95	1.43	0.69	1.20	1.19	2.04	1.29	2.07
	1.10	1.24	2.89	1.36	3.10	1.13	2.56	0.86	2.06	1.47	3.51	1.60	3.67
	1.26	1.40	4.29	1.47	4.57	1.18	3.74	0.94	3.00	1.56	5.07	1.71	5.38
	1.45	1.54	5.83	1.54	6.11	1.19	4.93	1.00	4.00	1.61	6.68	1.78	7.16
	1.66	1.77	7.60	1.75	7.86	1.35	6.28	1.14	5.14	1.78	8.46	2.03	9.19
	1.91	2.09	9.69	2.10	9.96	1.69	7.97	1.35	6.49	2.09	10.55	2.48	11.67

Continued

	2.19	2.41	12.10	2.47	12.43	2.08	10.05	1.57	8.06	2.41	12.96	2.95	14.62
	2.51	2.60	14.70	2.71	15.14	2.36	12.41	1.72	9.78	2.61	15.57	3.27	17.89
	2.88	2.66	17.36	2.79	17.93	2.50	14.91	1.80	11.58	2.69	18.26	3.41	21.30
	3.31	2.66	20.02	2.81	20.74	2.57	17.48	1.85	13.43	2.71	20.97	3.46	24.76
	3.80	2.69	22.71	2.83	23.57	2.65	20.13	1.94	15.37	2.77	23.74	3.54	28.30
	4.37	2.78	25.49	2.95	26.52	2.80	22.93	2.10	17.47	2.93	26.67	3.72	32.02
	5.01	2.94	28.43	3.16	29.68	3.03	25.96	2.35	19.82	3.20	29.87	4.01	36.03
	5.75	3.12	31.55	3.42	33.10	3.29	29.25	2.65	22.47	3.53	33.40	4.36	40.39
	6.61	3.26	34.81	3.63	36.73	3.47	32.72	2.96	25.43	3.82	37.22	4.64	45.03
	7.59	3.33	38.14	3.72	40.45	3.51	36.23	3.22	28.65	4.01	41.23	4.77	49.80
	8.71	3.37	41.51	3.73	44.18	3.43	39.66	3.46	32.11	4.13	45.36	4.77	54.57
	10.00	3.45	44.96	3.77	47.95	3.36	43.02	3.75	35.86	4.28	49.64	4.78	59.35
2 < Silt < 75	11.48	3.61	48.57	3.91	51.86	3.37	46.39	4.11	39.97	4.52	54.16	4.88	64.23
	13.18	3.75	52.32	4.12	55.98	3.41	49.80	4.49	44.46	4.80	58.96	4.98	69.21
	15.14	3.76	56.08	4.28	60.26	3.39	53.19	4.79	49.25	5.03	63.99	4.94	74.15
	17.38	3.56	59.64	4.33	64.59	3.28	56.47	4.97	54.22	5.14	69.13	4.70	78.85
	19.95	3.19	62.83	4.26	68.85	3.12	59.59	5.04	59.26	5.10	74.23	4.29	83.14
	22.91	2.70	65.53	4.08	72.93	2.95	62.54	4.99	64.25	4.86	79.09	3.75	86.89
	26.30	2.16	67.69	3.82	76.75	2.76	65.30	4.79	69.04	4.36	83.45	3.15	90.04
	30.20	1.63	69.32	3.52	80.27	2.56	67.86	4.43	73.47	3.65	87.10	2.55	92.59
	34.67	1.18	70.50	3.21	83.48	2.32	70.18	3.94	77.41	2.82	89.92	2.00	94.59
	39.81	0.91	71.41	2.93	86.41	2.05	72.23	3.40	80.81	2.03	91.95	1.55	96.14
	45.71	0.99	72.40	2.69	89.10	1.79	74.02	2.88	83.69	1.38	93.33	1.24	97.38
	52.48	1.50	73.90	2.46	91.56	1.56	75.58	2.41	86.10	0.90	94.23	1.02	98.40
	60.26	2.33	76.23	2.16	93.72	1.37	76.95	1.98	88.08	0.60	94.83	0.78	99.18
	69.18	3.20	79.43	1.81	95.53	1.27	78.22	1.66	89.74	0.51	95.34	0.52	99.70
	79.43	3.69	83.12	1.46	96.99	1.32	79.54	1.49	91.23	0.59	95.93	0.23	99.93
	91.20	3.54	86.66	1.15	98.14	1.50	81.04	1.44	92.67	0.72	96.65	0.06	99.99
	104.71	2.84	89.50	0.86	99.00	1.70	82.74	1.42	94.09	0.74	97.39	0.00	99.99
	120.23	2.12	91.62	0.61	99.61	1.72	84.46	1.32	95.41	0.60	97.99	0.00	99.99
	138.04	1.89	93.51	0.29	99.90	1.51	85.97	1.10	96.51	0.37	98.36	0.00	99.99
	158.46	2.17	95.68	0.10	100.00	1.24	87.21	0.82	97.33	0.21	98.57	0.00	99.99
	181.97	2.24	97.92	0.00	100.00	1.17	88.38	0.61	97.94	0.24	98.81	0.00	99.99
75 <	208.93	1.39	99.31	0.00	100.00	1.39	89.77	0.56	98.50	0.41	99.22	0.00	99.99
Sand <	239.88	0.38	99.69	0.00	100.00	1.62	91.39	0.58	99.08	0.46	99.68	0.00	99.99
4750	275.42	0.29	99.98	0.00	100.00	1.64	93.03	0.52	99.60	0.28	99.96	0.00	99.99
	316.23	0.02	100.00	0.00	100.00	1.55	94.58	0.32	99.92	0.01	99.97	0.00	99.99
	363.08	0.00	100.00	0.00	100.00	1.49	96.07	0.08	100.00	0.00	99.97	0.00	99.99
	416.87	0.00	100.00	0.00	100.00	1.44	97.51	0.01	100.01	0.00	99.97	0.00	99.99
	478.63	0.00	100.00	0.00	100.00	1.18	98.69	0.00	100.01	0.00	99.97	0.00	99.99
	549.54	0.00	100.00	0.00	100.00	0.69	99.38	0.00	100.01	0.00	99.97	0.00	99.99
	630.96	0.00	100.00	0.00	100.00	0.32	99.70	0.00	100.01	0.00	99.97	0.00	99.99
	724.44	0.00	100.00	0.00	100.00	0.19	99.89	0.00	100.01	0.00	99.97	0.00	99.99
	831.76	0.00	100.00	0.00	100.00	0.10	99.99	0.00	100.01	0.00	99.97	0.00	99.99

LP, P and L stand for study stations. E stands for collected samples, Cumul stands for cumulative granulometry.

In the fine particle fraction, silt is dominant with over 70% of the total sample (Figure 9). Silt is the dominant particles size reaching the Lom Pangar dam. This shows the bed of the reservoir being clogged. Clay varies between 6% to 12%. Thus the percentile D_{95} is insignificant as well as parameters SI, SKI, KG integrating it (Le Nindre & Serrano, 1988).

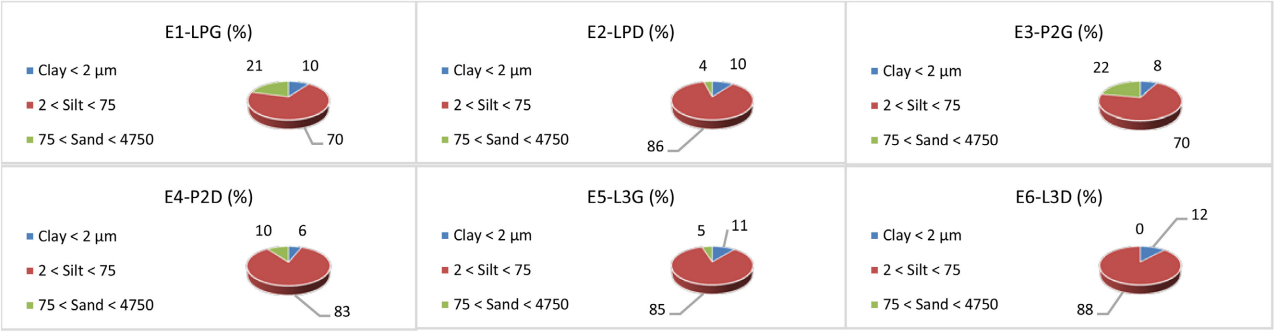

Figure 9. Proportion of fine particles of Lom Pangar Lacustrine and Transitional sections.

4.4. Granulometric Curves Analysis

Grain size curves are used to characterize the physical properties of sediments. They can provide information on the dynamics of geological and environmental processes.

- **Frequency curve**

The particularity of the Lom Pangar fine sediments is its multi-modal particle size distribution trend, presenting one major pic and many minor more or less shaped pics on the frequency curves (Figure 10).

For each curve the highest pics represents the major mode, indicating a class of the size where accumulated a maximum number of particle. There are many more individualized lower pics on each curve going from E6-L3D with 3 poorly individualized lower pics at the left of the mayor pic, to E1-LPG with 2 well individualized lower pics at the right of mayor pic. These lower pics indicate that particles size are differentiated and are likely accumulated on either size of the major pic to form minor modes of minor class sizes.

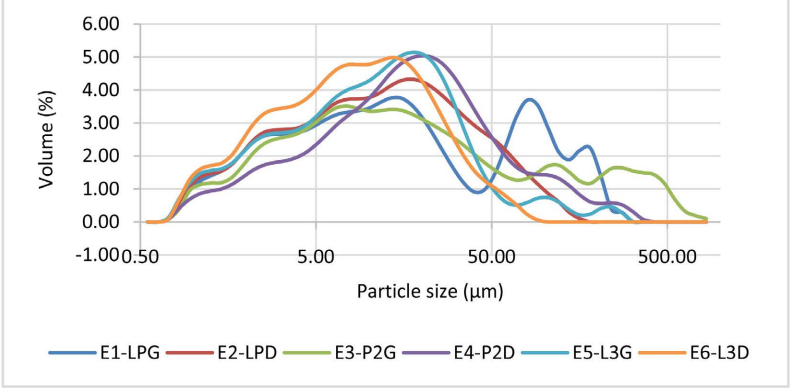

Figure 10. Particles size distribution frequency of Lom Pangar fine sediments.

This demonstrates the heterogeneity of sediments, indicated by a mixture of finer grains to sand, which corroborates with the relatively high uniformity parameter mentioned earlier. Such variability is a characteristic of fluvial sediments. The heterogeneity appears to be more pronounced in the right bank of the dam compared to the left bank.

- **Cumulative curve**

The cumulative curve of sediment granulometry is displayed on Figure 11.

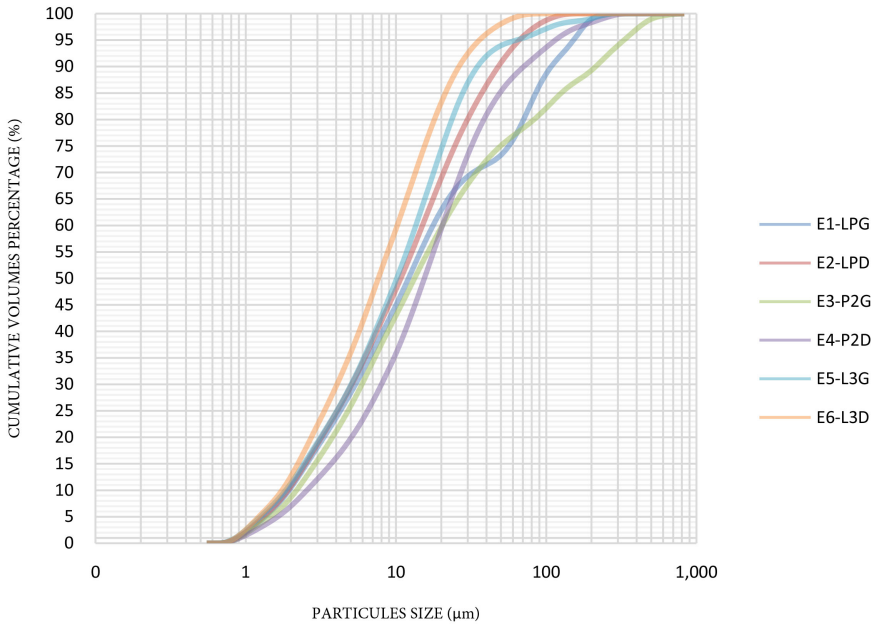

Figure 11. Cumulative curve of sediments granulometry of Lom Pangar.

It appears that all curves have the same trend with irregular highly stretched s-curve confirming the multi-modal frequency curve of the riverine sediments paleoenvironment. Samples from Pangar River tend to deviate at the top of the curve, indicating the relative coarse grain of that River branch.

4.5. Computing Indice Parameters

Various indices parameters characteristics are computed and displayed in Table 5. As mentioned in section 4, It more concerns elementary statistical analysis approaches, such as first and second statistical moments (mean, mode, skew and kurtosis) or percentiles (D_{50}, D_{84} … etc.). However, the theoretical basis for such use remains weak because these approaches assume a lognormal and unimodal Gaussian sedimentary distribution, which is rarely like in this case of Lom Pangar. Semi-quantitative indices like sorting indices (Trask index, Inman index, Folk and Ward index, etc.) are often temporary solutions and tend to be correlated with the standard deviation. Nevertheless, despite their limitations, central tendency values (mean, median), shape indices (skewness and kurtosis) and dispersion indices (sorting, etc.) remain dominant in the interpretation and graphical representation of particle size distributions (Duquesne & Carozza, 2023;

Folk, 1966; Fournier et al., 2014; Mercier, 2013).

Table 5. Computed indice parameters characterising Lom Pangar dam sediments.

Parameters	Formulae	E1-LPG	E2-LPD	E3-P2G	E4-P2D	E5-L3G	E6-L3D
Trask Index	Mean: $M_0 = (D_{25} + D_{75})/2$ (μm)	9.47	14.00	27.43	18.96	12.75	14.84
	S_0 = SQRT(D_{25}/D_{75})	0.53	0.41	0.31	0.45	0.42	0.36
	Skewness: $Sk = (D_{25} * D_{75})/D_{50} * D_{50}$ (μm)	61.908	96.00	242.5	201.915	85.785	88.894
Inman Index	Mean Phi: $M\Phi = (\Phi D_{16} + \Phi D_{84})/2$	−3.922	−3.317	−4.407	−3.774	−3.022	−2.787
	Standard Deviation Phi: $6\Phi = (\Phi D_{16} - \Phi D_{84})/2$	2.4621	1.91139	2.8219	1.780	1.694	1.542
	Skewness Phi: $Sk\Phi = (M\Phi - \Phi D_{50})/6\Phi$	−0.050	0.1625	−0.168	0.114	0.303	0.223
Krumbein Index	Quartile Deviation Phi: $QD\Phi = \log_{10}(S_0)$)	0.906	1.292	1.683	1.148	1.215	1.480

- **Dispersion parameters**

- **Trask Index mean M_0**

M_0 ranges from 9.47 at E1-LPG to 27.43 at E3-P2G. Values are low but relatively higher on the right bank of Pangar. It shows a lower spatial heterogeneity, indicating fewer differences between the D_{25} and D_{75} percentiles across the site. These values can be kept as a baseline to assess in the same condition, changes in spatial variability over time in the study areas keeping in mind that the right bank of the dam is relatively higher, due to the relatively short distance with the sediment source, compared to the Lom. This situation was also found in Osi River in southwestern of Nigeria (Lawal et al., 2017).

- **Sorting-Index S_0**

The sorting index S_0 ranges from 0.31 to 0.53 mm showing that sediments are very well sorted in the lacustrine and transitional sections of the Lom Pangar (Trask et al., 1932). According to the Trask sorting coefficient, this dispersion parameter is as worse as the value of S_0 is higher and parfait for values around 1, following the ranges of Table 6.

Table 6. Sorting-index classification coefficient.

$S_0 < 1.17$	very well sorted
$1.17 < S_0 < 1.20$	well sorted
$1.20 < S_0 < 1.35$	Fairly well sorted
$1.35 < S_0 < 1.87$	Medium sorted
$1.87 < S_0 < 2.75$	Poorly sorted
$2.75 < S_0$	Very poorly sorted

- **Inman Index Mean $M\Phi$**

As well as M_0, $M\Phi$ measures the heterogeneity of grain size within sediments. Negative values in Table 5 indicate a relatively uniform distribution of values across the study area with minimal variability between the lower D_{16} and upper D_{84} percentiles.

- **Heterometry index**

This is the Quartile Deviation Phi ($QD\Phi$) expressing how grain size varies within the sample. It refers to the variability of sediment properties across different spatial scales. It is determined by the Krumbein-Index with the Equation (3).

$$QD\Phi = \log_{10} S_0 \tag{3}$$

where S_0 is the Sorting-Index parameter.

For Lom Pangar, its value ranges from 0.906 to 1.683, confirming the low variability of the sediments grains size. This is explained by the well sorting particles found in the sorting index S_0.

- **Asymmetry parameter**

- **Skewness *Sk***

In addition to the position and dispersion parameters, the asymmetry parameter, measuring the shape of the distribution on either side of the median, is necessary for the correct definition of a particle size curve. For Trask-Index, Skewness *Sk* varies from 61.908 to 242.5 µm.

- **Skewness *Sk*Φ**

For the Inman Index, *Sk*Φ are very low and vary from −0.168 to 0.303 showing the high proposition of fine material in samples. Negative values correspond to dominance of finer sediments. The Inman Index also confirmed that sediments are fluviatile.

4.6. Tertiary Diagram

Particle size fractions were plotted on the Spark diagram (Figure 12).

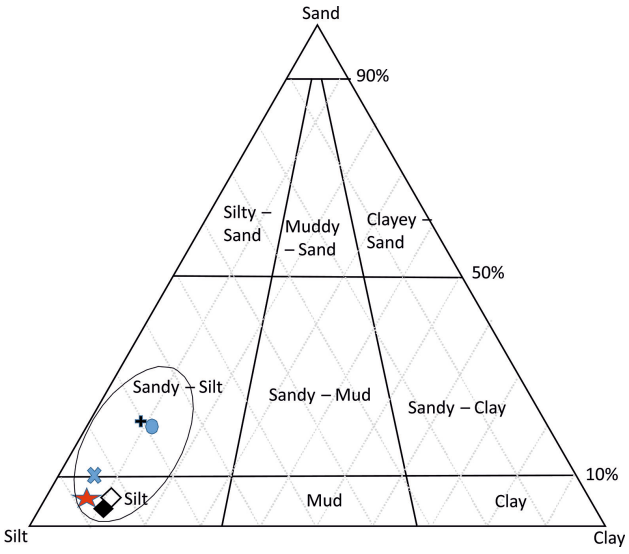

Figure 12. Particle size fractions of the Lom Pangar sediments in the Tertiary Spark diagram.

It appears that all sediments fall in the silted and sandy silted zone confirming the finer size of Lom Pangar sediments and corroborating with all previous pa-

rameters. As this method is based on arbitrary choices for class limits and sub-categories, it shows that categorization is simple and quick but works properly when dealing with samples of the same origin. If not it may become even challenging (Folk & Ward, 1957) in finding the most suitable texture classification scheme that maximizes the contrast between samples (Duquesne & Carozza, 2023).

5. Conclusion

This study was intended to assess the granulometric parameters of Lom Pangar sediments using samples collected from both riverine and transitional sections, employing standard methods. A diffusion Laser was used to analyze the particle's size and submitted to various particle characteristic parameters. Results indicate sediments heterogeneity, with 3 fractions: silts, larger than fine sand, and larger than clay. The sediments exhibit high sorting with low heterogeneity. These findings suggest the bottom of the reservoir may quickly become clogged. It also appears that the sandy fraction trend is higher in the right bank of the dam and can reach up to 22% on the right bank of the Pangar river. A fraction greater than 3000 μm is negligible. The management of the dam has to pay attention to these results as silts transportation may close the safety outlet of the dam, damage turbines, and provoke recurrent technical and safety issues. Additionally, the current clogging of the bottom of the reservoir may lead to an ecological problem with the limitation of the water exchanges with the underground water table, increase of sediments deposits and change in biogeochemistry processes.

Acknowledgements

Our acknowledgments go to the Romanian government and the "Agence Universitaire de la Francophonie (AUF)" as well as the "Electricity Development Cooperation (EDC)" of Cameroun, and Green Heart International for their support. It also go to Prof Alina Bădănoiu and team of the laboratory of Science and Engineering of Oxide Materials and Nanomaterials of the Politéhnica University of Bucharest in Romania.

Conflicts of Interest

The authors declare no conflicts of interest regarding the publication of this paper.

References

Abrahim, G. M. S., & Parker, R. J. (2008). Assessment of Heavy Metal Enrichment Factors and the Degree of Contamination in Marine Sediments from Tamaki Estuary, Auckland, New Zealand. *Environmental Monitoring and Assessment, 136,* 227-238. https://doi.org/10.1007/s10661-007-9678-2

Amarjouf, N., Hammadi, A., Oujidi, M., & Rezqi, H. (2015). Sedimentological, Geochemical and Morphoscopic Characterization of Sediments from Nador Harbor (Mo-

rocco) Caractérisations granulométrique, morphoscopique, minéralogique et géochimique des sédiments du port de Nador (Maroc). *Bulletin de l'Institut Scientifique, 36,* 1-11.

Antoine, G., Camenen, B., Jodeau, M., Némery, J., & Esteves, M. (2020). Downstream Erosion and Deposition Dynamics of Fine Suspended Sediments Due to Dam Flushing. *Journal of Hydrology, 585,* Article ID: 124763. https://doi.org/10.1016/j.jhydrol.2020.124763

Azrulhisham, E. A., & Azri, M. A. (2018). Application of LISST Instrument for Suspended Sediment and Erosive Wear Prediction in Run-of-River Hydropower Plants. In *2018 IEEE International Conference on Industrial Technology (ICIT)* (pp. 886-891). IEEE. https://doi.org/10.1109/ICIT.2018.8352295

Bai, J., Cui, B., Chen, B., Zhang, K., Deng, W., Gao, H., & Xiao, R. (2011). Spatial Distribution and Ecological Risk Assessment of Heavy Metals in Surface Sediments from a Typical Plateau Lake Wetland, China. *Ecological Modelling, 222,* 301-306. https://doi.org/10.1016/j.ecolmodel.2009.12.002

Bănăduc, D., Razvan, V., & Bănăduc, A. (2020). Sediments as Factor in the Fate of the Threatened Endemic Fish Species Romanichthys Valsanicola Dumitrescu, Bănărescu and Stoica, 1957 (Vâlsan River Basin, Danube Basin). *Transylvanian Review of Systematical and Ecological Research, 22,* 15-30. https://doi.org/10.2478/trser-2020-0008

Beck, H. E., Zimmermann, N. E., McVicar, T. R., Vergopolan, N., Berg, A., & Wood, E. F. (2018). Present and Future Köppen-Geiger Climate Classification Maps at 1-km Resolution. *Scientific Data, 5,* Article ID: 180214. https://doi.org/10.1038/sdata.2018.214

Bendaoud, A., Haddou, K., Taleb, A., & Belaidi, N. (2021). Assessment of Subsurface Riverbed Clogging by Fine Sediments in a Semi-Arid Catchment of North-Western Algeria. *African Journal of Aquatic Science, 46,* 54-66. https://doi.org/10.2989/16085914.2020.1719814

Bravard, J.-P., Goichot, M., & Tronchère, H. (2014). An Assessment of Sediment-Transport Processes in the Lower Mekong River Based on Deposit Grain Sizes, the CM Technique and Flow-Energy Data. *Geomorphology, 207,* 174-189. https://doi.org/10.1016/j.geomorph.2013.11.004

Chappell, A. (1998). Dispersing Sandy Soil for the Measurement of Particle Size Distributions Using Optical Laser Diffraction. *Catena, 31,* 271-281. https://doi.org/10.1016/S0341-8162(97)00049-0

Delanghe, D., Gairoard, S., Masson, M., & Le Bescond, C. (2017). *Méthodologie et intercomparaison des analyses granulométriques* (p. 64). INRAE. https://hal.science/hal-03379060

Duquesne, A., & Carozza, J.-M. (2023). Improving Grain Size Analysis to Characterize Sedimentary Processes in a Low-Energy River: A Case Study of the Charente River (Southwest France). *Applied Sciences, 13,* Article No. 8061. https://doi.org/10.3390/app13148061

EDC (2016). *Suivi de la qualité d'eau et des émissions de gaz à effet de serre de Lom Pangar*. Rapport Première année de remplissage, Electricity Developement Corporation.

Emadak, A., Acayanka, E., Nchimi Nono, K., Kamgang Youbi, G., Laminsi, S., & Fotie Lele, R. (2019b). Physicochemical Water Quality Assessment of the Lom River before the Commissioning of the Reservoir of the Lom Pangar Hydroelectric Dam in the East Region of Cameroon. In *4th Edition of Water, Energy and Environment (WEE), Congress* (11 p).

Emadak, A., Nsangou, T., Towa, A., Bell, E., & Ngouyamsa, H. N. (2019a). Environmental and Social Management of the Impoundment of the Reservoir of the Lom Pangar Hy-

droelectric Dam: Water Quality Monitoring. In *Africa 2019 Hydropower Conference* (17 p).

Folk, R. L. (1966). A Review of Grain-Size Parameters. *Sedimentology, 6,* 73-93. https://doi.org/10.1111/j.1365-3091.1966.tb01572.x

Folk, R. L., & Ward, W. C. (1957). Brazos River Bar [Texas]; a Study in the Significance of Grain Size Parameters. *Journal of Sedimentary Research, 27,* 3-26. https://doi.org/10.1306/74D70646-2B21-11D7-8648000102C1865D

Fournier, J., Gallon, R. K., & Paris, R. (2014). G2Sd: A New R Package for the Statistical Analysis of Unconsolidated Sediments. *Géomorphologie Relief Processus Environnement, 14,* 73-78. https://doi.org/10.4000/geomorphologie.10513

Fournier-Sowinski, J., Bonnot-Courtois, C., Paris, R., & Vot, M. (2012). *Analyses granulométriques. Principes et méthodes*.

Garnier-Laplace, J., Fournier-Bidoz, V., & Baudin, J. P. (1997). Etat des connaissances sur les échanges entre l'eau, les matières en suspension et les sédiments des principaux radionucléides rejetés en eau douce par les centrales nucléaires. *Radioprotection, 32,* 49-71. https://doi.org/10.1051/radiopro:1997103

Guillemot, T., Emadak, A., Lino, M., Daux, C., Coq, B., & Nsangou, T. (2017). The Lom Pangar Dam in Cameroon, from Design to Commissioning. In *Proceedings International Hydro Conference AFRICA 2017* (21 p).

Jain, C. K., Gupta, H., & Chakrapani, G. J. (2008). Enrichment and Fractionation of Heavy Metals in Bed Sediments of River Narmada, India. *Environmental Monitoring and Assessment, 141,* 35-47. https://doi.org/10.1007/s10661-007-9876-y

Kummu, M., Lu, X. X., Wang, J. J., & Varis, O. (2010). Basin-Wide Sediment Trapping Efficiency of Emerging Reservoirs along the Mekong. *Geomorphology, 119,* 181-197. https://doi.org/10.1016/j.geomorph.2010.03.018

Lawal, M., Grema, H. M., Ibrahim, H. A., Kitha, M., Yelwa, N. A., Abdullahi, I. M., & Muhammad, A. (2017). Determination of Origin and Granulometric Analysis of River Channel Sediments of Osi, Southwestern Nigeria. *Bayero Journal of Pure and Applied Sciences, 10,* 262-270. https://doi.org/10.4314/bajopas.v10i2.43

Le Nindre, Y. M., & Serrano, J. J. (1988). *Programme Granulo—Notice d'utilisation*. Bureau de Recherches Geologiques et Minieres-BP 6009-45060 Orleans. 51P; 88 SGN 126 Geo.

Li, F., Li, G., & Ji, J. (2011). Increasing Magnetic Susceptibility of the Suspended Particles in Yangtze River and Possible Contribution of Fly Ash. *Catena, 87,* 141-146. https://doi.org/10.1016/j.catena.2011.05.019

Li, M., Wilkinson, D., & Patchigolla, K. (2005). Comparison of Particle Size Distributions Measured Using Different Techniques. *Particulate Science and Technology, 23,* 265-284. https://doi.org/10.1080/02726350590955912

Mercier, J.-L. (2013). Indices granulométriques et lois de distributions. *Géomorphologie: Relief, Processus, Environnement, 19,* 379-392. https://doi.org/10.4000/geomorphologie.10357

Oehy (2003). *Effects of Obstacles and Jets on Reservoir Sedimentation Due to Turbidity Currents*. Ecole Polytechnique Federal de Lausanne.

Ousmanou, N. (2020). *Erosion and Sedimentation Impact on Storage Volume of Lom Pangar Hydroelectric Dam, Cameroon. Volume 6*.

Pélédé, S., Sako, A., & Bamba, O. (2018). Ecological Risk Assessment of Heavy Metals in Sediments from the Soubeira Reservoir, a Small-Scale Reservoir in North Central Burkina Faso, West Africa. *Environmental Pollution, 7,* 66-79.

https://doi.org/10.5539/ep.v7n1p66

Powell, A., & Soares Frazao, S. (2017). *Transport solide par charriage dans la rivière Cavaillon, Haïti*. Travail de fin d'études, UCL, Louvain-la-Neuve. https://dial.uclouvain.be/downloader/downloader.php?pid=thesis%3A8519&datastream=PDF_01

Pye, K., & Blott, S. J. (2004). Particle Size Analysis of Sediments, Soils and Related Particulate Materials for Forensic Purposes Using Laser Granulometry. *Forensic Science International, 144,* 19-27. https://doi.org/10.1016/j.forsciint.2004.02.028

Rai, A. K., Kumar, A., Staubli, T., & Yexiang, X. (2020). Interpretation and Application of the Hydro-Abrasive Erosion Model from IEC 62364 (2013) for Pelton Turbines. *Renewable Energy, 160,* 396-408. https://doi.org/10.1016/j.renene.2020.06.117

Rivière, A. (1977). *Méthodes Granulométriques-Techniques et Interprétations*. https://trid.trb.org/View/1058243

Schleiss, A., De Cesare, G., & Jenzer Althaus, J. (2008). *Reservoir Sedimentation and Sustainable Development*. CHR Workshop Erosion, Transport and Deposition of Sediments, CONF. https://infoscience.epfl.ch/record/125169/files/2008-593_Reservoir%20sedimentation%20and%20sustainable%20development.pdf

Schmutz, S., & Moog, O. (2018). Dams: Ecological Impacts and Management. In S. Schmutz, & J. Sendzimir (Eds.), *Riverine Ecosystem Management: Science for Governing towards a Sustainable Future* (pp. 111-127). Springer.

Seliger, C., & Zeiringer, B. (2018). Riverine Ecosystem Management Science for Governing Towards a Sustainable Future. In S. Schmutz, & J. Sendzimir (Eds.), *Riverine Ecosystem Management: Science for Governing towards a Sustainable Future* (pp. 171-186). Springer.

Sharma, S., & Gandhi, B. K. (2023). Assessment of Erosion Wear in Low Specific Speed Francis Turbine Due to Particulate Flow. *Advanced Powder Technology, 34,* Article ID: 104065. https://doi.org/10.1016/j.apt.2023.104065

Sharma, S., Gandhi, B. K., & Pandey, L. (2021). Measurement and Analysis of Sediment Erosion of a High Head Francis Turbine: A Field Study of Bhilangana-III Hydropower Plant, India. *Engineering Failure Analysis, 122,* Article ID: 105249. https://doi.org/10.1016/j.engfailanal.2021.105249

Singh, J. (2021). Application of Thermal Spray Coatings for Protection against Erosion, Abrasion, and Corrosion in Hydropower Plants and Offshore Industry. In L. Thakur, & H. Vasudev (Eds.), *Thermal Spray Coatings* (41 p). CRC Press.

Suresh, G., Sutharsan, P., Ramasamy, V., & Venkatachalapathy, R. (2012). Assessment of Spatial Distribution and Potential Ecological Risk of the Heavy Metals in Relation to Granulometric Contents of Veeranam Lake Sediments, India. *Ecotoxicology and Environmental Safety, 84,* 117-124. https://doi.org/10.1016/j.ecoenv.2012.06.027

Swartenbroekx, C., Zech, Y., & Soares-Frazão, S. (2013). Two-Dimensional Two-Layer Shallow Water Model for Dam Break Flows with Significant Bed Load Transport. *International Journal for Numerical Methods in Fluids, 73,* 477-508. https://doi.org/10.1002/fld.3809

Tandel, R. R., Patel, R. N., & Jain, S. V. (2023). Correlation Development of Erosive Wear and Silt Erosion Failure Mechanisms for Pump as Turbine. *Engineering Failure Analysis, 153,* Article ID: 107610. https://doi.org/10.1016/j.engfailanal.2023.107610

Tarodiya, R., Khullar, S., & Levy, A. (2022). Particulate Flow and Erosion Modeling of a Pelton Turbine Injector Using CFD-DEM Simulations. *Powder Technology, 399,* Ar-

ticle ID: 117168. https://doi.org/10.1016/j.powtec.2022.117168

Taylor, M. P. (2007). Distribution and Storage of Sediment-Associated Heavy Metals Downstream of the Remediated Rum Jungle Mine on the East Branch of the Finniss River, Northern Territory, Australia. *Journal of Geochemical Exploration, 92,* 55-72. https://doi.org/10.1016/j.gexplo.2006.07.005

Touchette, M., Cloutier, C.-A., Buffin-Bélanger, T., Chaillou, G., Hétu, B., Lewis, N., & McCormack, R. (2015). *Programme d'acquisition de connaissances sur les eaux souterraines du nord-est du Bas-Saint-Laurent (PACES-NEBSL) Rapport Final.*

Trask, P. D., Hammar, H. E., & Wu, C. (1932). *Origin and Environment of Source Sediments of Petroleum*. Printed by the Gulf Pub. Co.

Vörösmarty, C. J., Meybeck, M., Fekete, B., Sharma, K., Green, P., & Syvitski, J. P. M. (2003). Anthropogenic Sediment Retention: Major Global Impact from Registered River Impoundments. *Global and Planetary Change, 39,* 169-190. https://doi.org/10.1016/S0921-8181(03)00023-7

Wanogho, S., Gettinby, G., & Caddy, B. (1987). Particle Size Distribution Analysis of Soils Using Laser Diffraction. *Forensic Science International, 33,* 117-128. https://doi.org/10.1016/0379-0738(87)90147-2

Whitaker, A. C., & Potts, D. F. (2007). Coarse Bed Load Transport in an Alluvial Gravel Bed Stream, Dupuyer Creek, Montana. *Earth Surface Processes and Landforms, 32,* 1984-2004. https://doi.org/10.1002/esp.1512

White, J., Jegat, V., Van Lancker, V., Deleu, S., & Vanstaen, K. (2007). Multibeam Echo Sounders. In R. Coggan, et al. (Eds.), *Review of Standards and Protocols for Seabed Habitat Mapping* (pp. 53-72). MESH.

White, W., Meyer Peter, E., Rottner, J., Ackers, P., Milli, H., Muller, R., Bishop, A., Hansen, E., Crabbe, A., Einstein, H., Bangold, R., & Toffaleti, F. (1975). Sediment Transport Theories. *Proceedings of the Institution of Civil Engineers, 59,* 265-292. https://doi.org/10.1680/iicep.1975.3740